Atmospheric Correction of AMSR-E Brightness Temperatures for Dry Snow Cover Mapping

Marco Tedesco and James R. Wang

***Abstract*—Differences between the brightness temperatures (*spectral gradient*) collected by the Advanced Microwave Scanning Radiometer for EOS (AMSR-E) at 18.7 and 36.5 GHz are used to map the snow-covered area (SCA) over a region including the western U.S. The brightness temperatures are corrected to take into account for atmospheric effects by means of a simplified radiative transfer equation whose parameters are stratified using rawinsonde data collected from a few stations. The surface emissivity is estimated from the model, and the brightness temperatures at the surface are computed as the product of the surface temperature and the computed emissivity. The SCA derived from microwave data is compared with that obtained from the Moderate Resolution Imaging Spectroradiometer for both cases of corrected and noncorrected brightness temperatures. The improvement to the SCA retrievals based on the corrected brightness temperatures shows an average value around 7%.**

***Index Terms*—Atmospheric correction, microwave, remote sensing, snow.**

I. Introduction

SNOW affects the hydrological, meteorological, and climatological cycles through its effects on land surface albedo, the net radiation balance, and boundary layer stability. In many high-latitude and mountainous regions of the Earth the majority of total annual precipitation occurs as snowfall [1], and many rivers originate from melting snow, which represents a major source of fresh water. Global mapping of snow parameters and snow-covered area (SCA) is crucial to understand the evolution of the cryosphere for quantifying the water resources and improving the global climate and hydrological models. Satellite remote sensing is an appealing tool for mapping the extent of hemispheric SCA over large areas where, otherwise, it would be difficult if not impossible. Data collected in the visible region offer high spatial resolution. However, temporal resolution of optical data is limited by clouds presence and solar illumination. Microwave signals are not dependent on clouds and solar illumination, guaranteeing high temporal resolution, but data are collected at a coarse spatial resolution. The SCA maps can be derived from the pixels where the values of snow depth (SD) or snow water equivalent (SWE) are greater than zero. Several algorithms have been developed during the past years for their retrieval from spaceborne radiometric data [2]–[5]. Some of these algorithms (e.g., [2]) are based on the volumetric scattering induced by dry snow and make use of linear relationships relating the SWE (or snow depth) to the difference between the 19- and 37-GHz (or similar frequencies) brightness temperatures.

The presence of the atmosphere must be considered when dealing with satellite data. The microwave signal at the surface passes through the atmosphere before being detected by a spaceborne sensor, and thus it is subject to the effects of atmospheric absorption and emission. Although these effects are small at the frequencies of interest (19 and 37 GHz, or similar frequencies), the brightness temperatures at the two frequencies are affected in a different manner. As a consequence, the spectral gradient (defined as the difference between the 19- and 37-GHz brightness temperatures) obtained from spaceborne data can be different from that one obtained using brightness temperatures at the surface.

In this study, we use the difference between the brightness temperatures at 18.7 and 36.5 GHz recorded by the Advanced Microwave Scanning Radiometer for EOS (AMSR-E) to map SCA over an area located in the western U.S. The radiometric data are corrected for atmospheric effects by means of a radiative transfer model. Results are reported for a period of interest between October 2003 and April 2004. Detailed maps of the results regarding two dates (March 9, March 25, 2004) are also reported. The SCA derived from microwave data in both cases of corrected and noncorrected brightness temperatures are compared with daily SCA product derived from Moderate Resolution Imaging Spectroradiometer (MODIS), and the differences are discussed.

The letter is structured as follows. In Section II, we describe the area of interest, together with the microwave and optical data. Section III describes the methodology adopted for the correction of the brightness temperatures and the procedure adopted for the comparison of the SCA derived from microwave and optical data. In Section IV we show the results, and in the last section we report our conclusions.

II. Area of Interest and the Microwave and Optical Data

The area of interest is located in the western U.S. (36° to 48°N, 103° to 126°W), and it includes the Sierra Nevada. This area is subject of several investigations, and it is of crucial importance because the snow here accumulated during the winter time serves as storage of fresh water for many surrounding areas, supplying two-thirds of California's water and most of the water for northern Nevada.

Microwave data consist of AMSR-E Level 2A (L2A) brightness temperatures at 18.7 and 36.5 GHz. The L2A product pro-

Manuscript received July 11, 2005; revised November 1, 2005.

M. Tedesco is with the Goddard Earth Sciences and Technology Center, University of Maryland Baltimore County, Baltimore, MD 21228 USA and also with the NASA Goddard Space Flight Center, Greenbelt, MD 20771 USA (e-mail: mtedesco@umbc.edu)..

J. R. Wang is with the Hydrospheric and Biospheric Processes Laboratory, NASA Goddard Space Flight Center, Greenbelt, MD 20771 USA.

Digital Object Identifier 10.1109/LGRS.2006.871744

vides brightness temperatures resampled to be spatially consistent and available at a variety of resolutions, corresponding to the footprint size of the observations (http://nsidc.org/data/docs/daac/ae_l2a_tbs.gd.html). The resolution used in this study is 21 km. This choice is forced by the resolution of the 18.7-GHz channel. Only data from descending passes (night time) are used in this study as the SWE retrieval algorithm works properly only for dry snow conditions. Indeed, when snow melts, the penetration depth strongly decreases as a consequence of the increased absorption (wetness) at both 18.7 and 36.5 GHz. Brightness temperatures also increase and the spectral difference reduces as the brightness temperatures at the two frequencies get closer. As wetness increases, the spectral gradient is less sensitive to SWE, and it is, therefore, required to minimize the number of pixels where wet snow is present.

Optical data consist of SCA derived form the MODIS/Aqua Snow Cover Daily L3 Global 500-m Grid product (MYD10A1) [6]. The MODIS product contains snow cover and quality assurance (QA) data in HDF-EOS format, along with corresponding metadata. Each granule consists of 1200 km × 1200 km tiles of 500-m resolution data gridded in a sinusoidal map projection.[1]

III. Methodology

In this section, we report the method used to correct the brightness temperatures and the techniques used to retrieve the SCA from microwave satellite data and compare it with the optical data.

A. Correction of Brightness Temperatures

The brightness temperatures (T_b) observed by the AMSR-E depend on the effective atmospheric temperature (T_a), optical depth (τ), surface emissivity (e), and surface temperature (T_s). At frequency ν, incidence angle θ, and polarization p brightness temperature can be approximated by [7]

$$\begin{aligned} T_{bp}(\nu,\theta) &= T_a(\nu,\theta)\cdot\left(1-e^{-\tau(\nu,\theta)}\right)+e^{-\tau(\nu,\theta)} \\ &\quad\cdot\left[e_p(\nu,\theta)\cdot T_s+(1-e_p(\nu,\theta))\cdot T_a(\nu,\theta)\right. \\ &\quad\left.\cdot\left(1-e^{-\tau(\nu,\theta)}\right)\right]+(1-e_p(\nu,\theta)) \\ &\quad\cdot T_{CB}\cdot e^{-2\tau(\nu,\theta)} \\ &= T_a(\nu,\theta)\cdot(1-\Gamma(\nu,\theta))+\Gamma \\ &\quad\cdot\left[e_p(\nu,\theta)\cdot T_s+(1-e_p(\nu,\theta))\cdot T_a(\nu,\theta)\right. \\ &\quad\left.\cdot(1-\Gamma(\nu,\theta))\right] \\ &\quad+(1-e_p(\nu,\theta))\cdot T_{CB}\cdot\Gamma(\nu,\theta)^2 \end{aligned} \tag{1}$$

where T_{CB} is the cosmic background radiation and the absorption factor is written as $\Gamma(\nu,\theta)=e^{-\tau(\nu,\theta)}$. Thus, the emissivity at the surface can be expressed as

$$\begin{aligned} &e_p(\nu,\theta) \\ &=\frac{T_{bp}(\nu,\theta)-T_a(\nu,\theta)+[T_a(\nu,\theta)-T_{CB}]\cdot\Gamma(\nu,\theta)^2}{[T_s-T_a(\nu,\theta)+T_a(\nu,\theta)\cdot\Gamma(\nu,\theta)-T_{CB}\cdot\Gamma(\nu,\theta)]\cdot\Gamma(\nu,\theta)} \end{aligned} \tag{2}$$

with $\tau(x,y,\nu,\theta)=\int_x^y\gamma(\nu,z)\cdot\sec\theta\cdot dz/(\gamma(\nu,z)$ being the absorption coefficient of the atmosphere) and $T_a(\nu,\theta)=(\int_0^\infty e^{-\tau(0,z,\nu,\theta)}\cdot T(z)\cdot\gamma(\nu,z)\cdot\sec\theta\cdot dz)/\int_0^\infty e^{-\tau(0,z,\nu,\theta)}\cdot\gamma(\nu,z)\cdot\sec\theta\cdot dz$ with $T(z)$ being the atmospheric temperature profile. To stratify T_a and τ, three months (December 2003–February 2004) of rawinsonde data from three widely separated stations (Oakland, Lake Tahoe, and Twin City) are acquired. The atmospheric absorption model of Rosenkranz [8] is used in the calculations of T_a and τ. These parameters at 18.7 and 36.5 GHz are not sensitive to moisture variations but can be shown to depend on elevation [9]. To simplify the correction procedure for the large AMSR-E footprints we assumed an average elevation of 1 km and calculated the average T_a and τ from the three rawinsonde data sets for the entire region. The standard deviations for T_a and absorption factor $\exp(-\tau)$ calculated from these rawinsonde data are about ±3.7 K and 0.004, respectively, which would not introduce much error in the T_b estimation [9]. We calculate the surface emissivity e from each available pixel by means of the (2). The AMSR-E brightness temperatures T_b and land surface temperatures T_s (obtained from the MODIS Land Surface Temperature product) are colocated and the surface brightness temperature is then obtained by the product of e and T_s. For brightness temperature gradient calculations (e.g., Fig. 2), the input T_s values are not critical because they apply to both 18.7 and 36.5 GHz. Further details about the procedure applied can be found in [7] and [9].

B. Snow-Covered Areas From Microwave and Optical Data

The formula used for calculating the SWE from microwave data is

$$\mathrm{SWE}=a*(\mathrm{Tb}_{18.7V}-\mathrm{Tb}_{36.5V}) \tag{3}$$

where the coefficient a depends on snow particle size, and it is here set to 4.8 [2]. In order to assure dry snow conditions, a threshold value of 255 K is used for the 36.5-GHz brightness temperatures [10], [11]. All pixels having brightness temperatures greater than 255 K are, therefore, systematically disregarded. The SCA is, then, derived from those pixels having an SWE greater than zero.

The MODIS SCA data are resampled at 21-km resolution from the original 500-m resolution. This is done through the software MODIS Reprojection Tool (MRT).[2] The resampling procedure of the MODIS product can lead to errors due to pixel aggregation. For the area under study, the regions covered by snow are well separated from the regions free of snow, and this helps to reduce the error due to resampling. The relative percentage error due to the resampling process has been quantified in other studies [12]. Results show that the average error and standard deviation due to the resampling from 0.5 to 21 km are, respectively, 0.151% and 0.87%, with a maximum absolute average error around 4%.

The MODIS- and AMSR-E-derived SCA are coregistered by means of an IDL software developed for this purpose. The coregistration error (the distance between the coordinated of the

[1]Further information about the MODIS SCA product here used can be found at http://nsidc.org/data/docs/daac/mod10a1_modis_terra_snow_daily_global_500m_grid.gd.html.

[2]http://edcdaac.usgs.gov/landdaac/tools/modis/index.asp

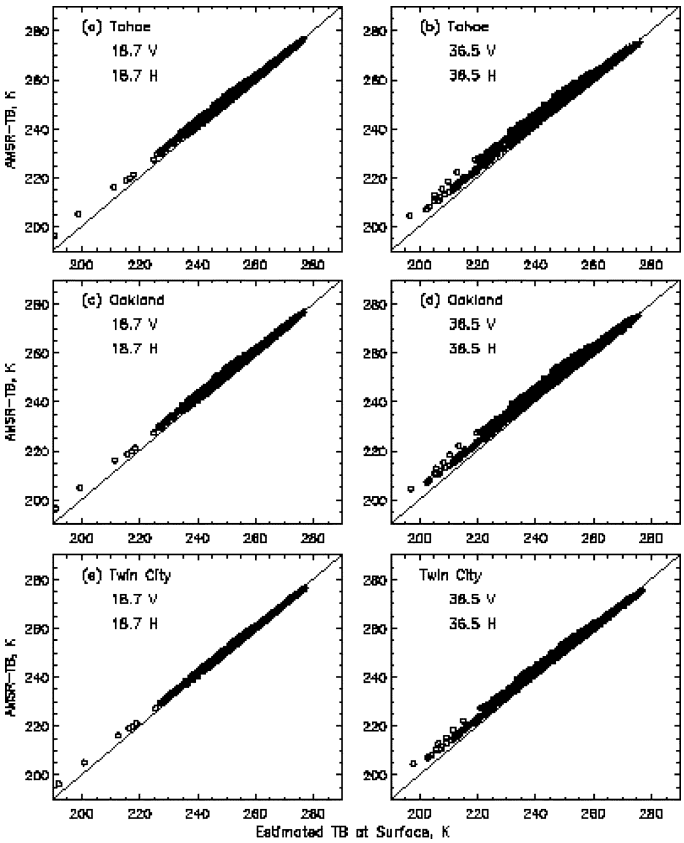

Fig. 1. Brightness temperatures at 18.7 and 36.5 GHz estimated at the surface versus brightness temperatures recorded by AMSR-E for the three selected locations of Tahoe, Oakland, and Twin City.

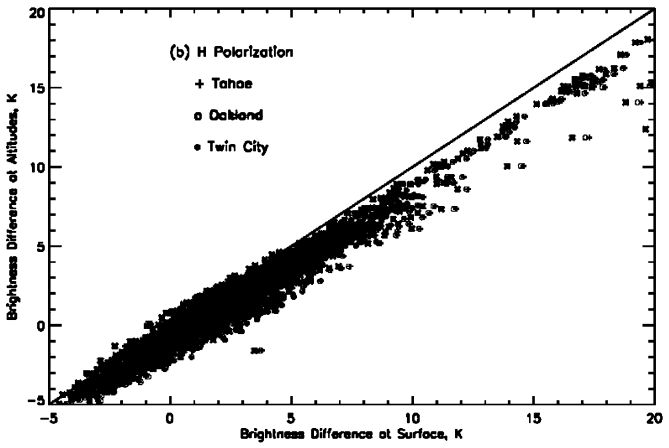

Fig. 2. Difference between brightness temperatures 18.7 and 36.5 GHz estimated at the surface versus difference between brightness temperatures recorded by AMSR-E for the area under study.

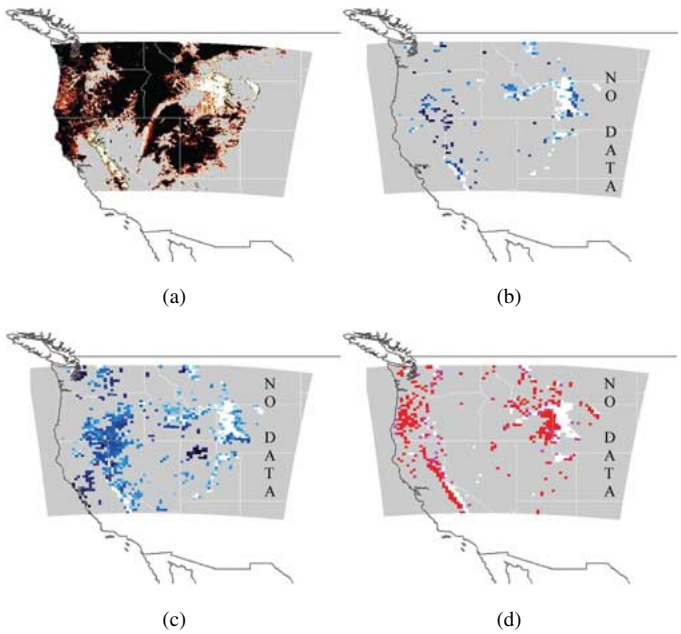

Fig. 3. Results and data for March 9, 2004. (a) Distribution of cloud and snow cover areas derived from MODIS. Black corresponds to clouds and white to snow. (b) SWE derived from noncorrected AMSR-E brightness temperatures (blue corresponds to low values and white to high values of SWE). (c) Same as (b) but from corrected AMSR-E brightness temperatures. (d) RGB composite image with red = MODIS SCA, green = SCA derived from uncorrected AMSR-E brightness temperatures and blue = SCA derived from corrected AMSR-E brightness temperatures.

center of the pixel for the MODIS and AMSR-E products) is estimated to be 1.5 km along the longitude and 3 km along the latitude.

IV. Results and Discussion

Fig. 1 shows the brightness temperatures estimated at the surface versus those acquired by the AMSR-E for the three selected locations of Tahoe (39.57°N, 119.80°W), Oakland (37.75°N, 122.22°W), and Twin City (44.83°N, 93.55°W). From the figure, we observe that the AMSR-E brightness temperatures at 18.7 and 36.5 GHz are, in general, higher than those ones estimated at the surface. The differences between surface-estimated and satellite brightness temperatures increases as brightness temperatures decrease. Fig. 2 shows the spectral gradient at the surface versus that obtained from the AMSR-E data, horizontal polarization. Results show that the difference between corrected and uncorrected values of the spectral gradient increases as the spectral gradient increases. It follows that if the atmospheric effects are not taken into account the SCA retrieved using spaceborne brightness temperatures can be smaller than the area retrieved using surface estimated brightness temperatures. The maximum observed difference between the spectral gradients computed from uncorrected and corrected brightness temperatures is around 6 K.

In Figs. 3 and 4, we show the comparison between the SCA derived from optical data and from microwave data for March 9, and March 24, 2004. In each figure we show (a) distribution of cloud and snow cover areas derived from MODIS (with black color corresponding to clouds and white color to snow), (b) SWE derived from uncorrected AMSR-E brightness temperatures (with blue color corresponding to low values of SWE and white to high values of SWE), (c) SWE derived from corrected AMSR-E brightness temperatures (also with blue corresponding to low values of SWE and white to high values of SWE), and (d) RGB composite image with red = MODIS SCA, green = SCA derived from uncorrected AMSR-E brightness temperatures and blue = SCA derived from corrected AMSR-E brightness temperatures. In the RGB image, red color represents the SCA obtained by MODIS but

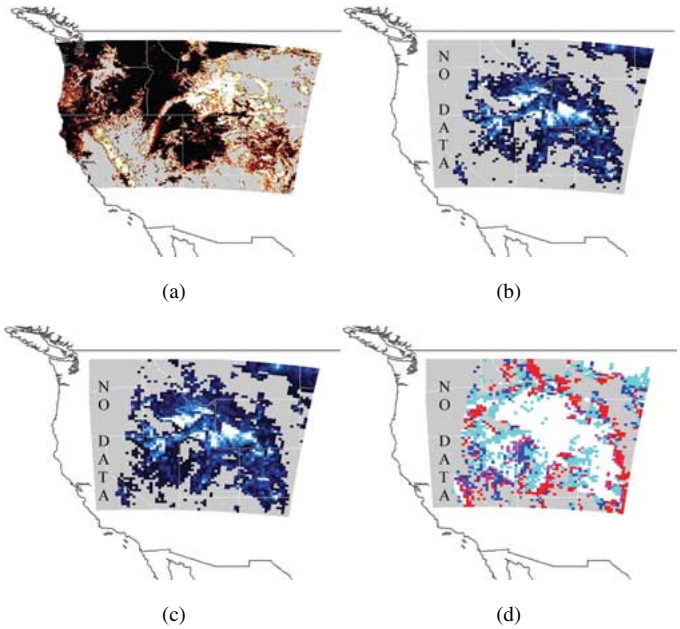

Fig. 4. Results and data for March 25, 2004. (a) Distribution of cloud and snow cover areas derived from MODIS. Black corresponds to clouds and white to snow. (b) SWE derived from noncorrected AMSR-E brightness temperatures (blue corresponds to low values and white to high values of SWE). (c) Same as (b) but from corrected AMSR-E brightness temperatures. (d) RGB composite image with red = MODIS SCA, green = SCA derived from uncorrected AMSR-E brightness temperatures and blue = SCA derived from corrected AMSR-E brightness temperatures.

not detected by AMSR-E (both corrected and uncorrected brightness temperatures). Purple represents the SCA detected by using the corrected brightness temperatures matching by MODIS, white represents the SCA detected by MODIS and AMSR-E (both corrected and uncorrected brightness temperature). Fig. 5 plots the temporal trend of snow pixels detected by MODIS, expressed as percentage of snow pixels over the total number of pixels, and percentage of snow pixels detected by AMSR-E with atmospheric correction, expressed as the ratio between the number of snow pixels detected by AMSR-E over the number of snow pixels detected by MODIS ($N_{\text{snow\_AMSR-E\_corr}}/N_{\text{snow\_MODIS}}$) between October 2003 and April 2004. In Table I, we also report the total number of pixels (N_{TOT}), the number of pixels classified by MODIS as covered by snow (N_{MODIS}) and the percentage of pixels classified as covered by snow using uncorrected ($N_{\text{AMSR-E}}$) and corrected microwave data ($N_{\text{AMSR-E\_CORR}}$) relative to the MODIS SCA pixels. In the table, the results regarding the data of the cases plotted in Figs. 3 and 4 are reported together with the average values obtained for the period October 2003–April 2004. The last column reports the difference between the results obtained using corrected and uncorrected brightness temperatures. The relative improvement due to the atmospheric correction is 9.63% on March 9 and 12.93% on March 24, 2003. The average relative improvement over the period October 2003–April 2004 is 6.77%.

V. Conclusion

The difference between the brightness temperatures at 18.7 and 36.5 GHz collected by the AMSR-E were used to map

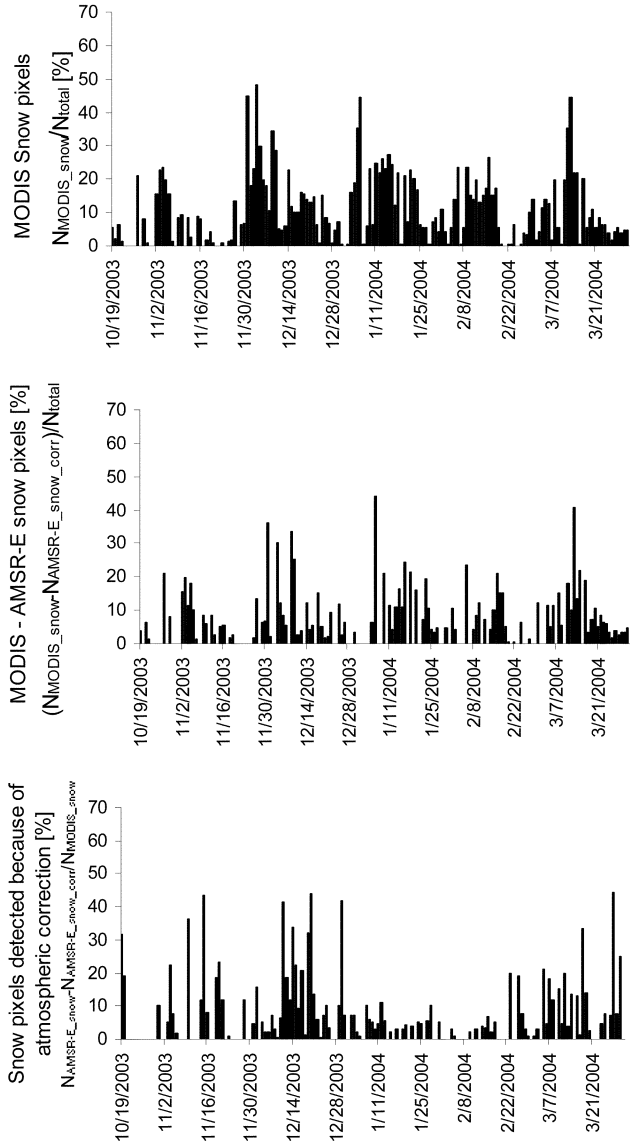

Fig. 5. Temporal behavior of percentage ($N_{\text{MODIS\_snow}}/N_{\text{total}}$) of snow pixels detected by MODIS (top), difference between percentage of snow cover pixels ($N_{\text{MODIS\_snow}}/N_{\text{total}} - N_{\text{AMSR-E\_snow\_corr}}/N_{\text{total}}$) obtained with MODIS and AMSR-E corrected brightness temperatures (middle), and percentage of SNOW pixels detected by AMSR-E due to the atmospheric correction ($\{N_{\text{AMSR-E\_snow\_corr}} - N_{\text{AMSR-E\_snow}}\}/N_{\text{MODIS\_snow}}$) (bottom) between October 2003 and April 2004.

snow-covered areas over a region in the western U.S. The brightness temperatures were corrected for the atmospheric effects using a radiative transfer approach where the input parameters were obtained from rawinsonde data. Results show that the AMSR-E brightness temperatures at 18.7 and 36.5 GHz are higher than those estimated at the surface. The difference between surface-estimated and satellite-based brightness temperatures increases as the brightness temperatures decrease. The values of the spectral gradient for the corrected brightness temperatures are, in general, higher than those of the uncorrected brightness temperatures. The maximum difference between the values of spectral gradients computed from uncorrected and corrected brightness temperatures is around 6 K.

TABLE I
TOTAL NUMBER OF PIXELS (N_{TOT}), THE NUMBER OF PIXELS CLASSIFIED BY MODIS AS COVERED BY SNOW (N_{MODIS}), AND THE NUMBER OF PIXELS CLASSIFIED AS COVERED BY SNOW USING UNCORRECTED ($N_{\mathrm{AMSR-E}}$) AND CORRECTED MICROWAVE DATA ($N_{\mathrm{AMSR-E\_CORR}}$) MATCHING THE MODIS DATA FOR EACH DATE

Date	N_{total}	$N_{MODIS\text{-}SNOW}$	$N_{AMSR\text{-}E\_SNOW}$	$N_{AMSR\text{-}E\_SNOW\_CORR}$	Difference
March 9, 2004	3562	1735	1171 (67.49 %)	1338 (77.12 %)	9.63 %
March 25, 2004	4445	549	172 (31.33 %)	243 (44.26 %)	12.93 %
Oct. 2003 – Apr. 2004 (Average)	4106	613	250 (40.87 %)	292 (47.64 %)	6.77 %

The SCA derived from both uncorrected and corrected microwave data were compared with those obtained from MODIS. Results show that the number of SCA pixels derived from microwave data matching the SCA MODIS pixels is higher when the corrected brightness temperatures are used. As a consequence, accounting for the atmospheric effects can improve the retrievals of SCA from the microwave observations. The improvement deriving from using values of corrected brightness temperatures was expressed in terms of the difference between the percentage of number of pixels derived using AMSR-E brightness temperatures over the number of pixels classified as snow by MODIS. The average value of this difference for the season 2003–2004 was found to be 6.77%, with maximum values around 40%.

Future study will include the development of a rigorous approach to the atmospheric corrections (e.g., taking into account the effect of elevation) and the extension of this analysis to other periods and areas of interest.

ACKNOWLEDGMENT

The authors wish to thank Jeff Miller (SSAI) for his support for developing and adapting the software used in this study and for the many discussions on the improvement of the letter. The authors would also like to thank the anonymous reviewers and the associate editors for the many useful suggestions.

REFERENCES

[1] D. Robinson, K. Dewey, and R. Heim, "Global snow cover monitoring: An update," *Bull. Amer. Meteorol. Soc.*, vol. 74, pp. 1689–1696, 1993.
[2] A. T. C. Chang, J. L. Foster, and D. K. Hall, "1987: Nimbus-7 SMMR derived global snow cover parameters," *Ann. Glaciol.*, vol. 9, pp. 39–4.
[3] J. Pulliainen and M. Hallikainen, "Retrieval of regional snow water equivalent from space-borne passive microwave observations," *Remote Sens. Environ.*, vol. 75, pp. 76–8, 2001.
[4] R. Kelly, A. T. Chang, L. Tsang, and J. L. Foster, "A prototype AMSR-E global snow area and snow depth algorithm," *IEEE Trans. Geosci. Remote Sens.*, vol. 41, no. 2, pp. 230–242, Feb. 2003.
[5] M. Tedesco, J. Pulliainen, P. Pampaloni, and M. Hallikainen, "Artificial neural network based techniques for the retrieval of SWE and snow depth from SSM/I data," *Remote Sens. Environ.*, vol. 90, no. 1, pp. 76–8, 2004.
[6] D. K. Hall, G. A. Riggs, and V. V. Salomonson, "MODIS/Aqua Snow Cover Daily L3 Global 500 m Grid V004, January to March," Nat. Snow and Ice Data Center, Boulder, CO, 2003, Updated daily.
[7] J. R. Wang and W. Manning, "Near concurrent MIR, SSM/T-2, and SSM/I observations over snow-covered surfaces," *Remote Sens. Environ.*, vol. 84, no. 3, pp. 457–470, Feb. 2003.
[8] P. W. Rosenkranz, "Water vapor microwave continuum absorption: A comparison of measurements and models," *Radio Sci.*, vol. 33, pp. 919–928, 1998.
[9] J. R. Wang, P. E. Racette, J. E. Pieppmeier, B. Monosmith, and W. Manning, "CoSMIR measurements of precipitable water and surface emissivities over snow-covered Sierra mountains," *IEEE Trans. Geosci. Remote Sens.*, submitted for publication.
[10] A. T. C. Chang and A. Rango, Algorithm Theoretical Basis Document (ATBD) for the AMSR-E Snow Water Equivalent Algorithm NASA Goddard Space Flight Center. Greenbelt, MD, 2000 [Online]. Available: http://eospso.gsfc.nasa.gov/ftp_ATBD/REVIEW/AMSR/atbd-amsr-snow.pdf
[11] R. Kelly, private communication.
[12] M. Tedesco, J. R. Wang, R. J. Kelly, and D. K. Hall, "Inter-comparison of optical and microwave remote sensing derived snow products and ground validation," presented at the *Eur. Geosciences Union, General Assembly*, Vienna, Austria, Apr 24–29, 2005.